Available online at www.sciencedirect.com

ScienceDirect

ARTICLE

Effect of Mischmetal on Microstructure and Mechanical Properties of Superlight Mg-Li Alloys

Li Yangmin[1], Peng Xiaodong[1,2], Hu Faping[1], Wei Guobing[1], Xie Weidong[1,2], Liu Junwei [1], Yang Yan[1], Li Mengluan[1], Wang Xuemei[3]

[1] College of Materials Science and Engineering, Chongqing University, Chongqing 400044, China; [2] National Engineering Research Center for Magnesium Alloys, Chongqing 400044, China; [3] Saic-iveco Hongyan Commercial Vehicle Co, LTD, Chongqing 401122, China

Abstract: The influence of mischmetal (lanthanum and cerium) on the microstructure and mechanical properties of Mg-9Li-3Al-xRE (x=0, 0.5, 1, 1.5, 2, wt%) alloys was investigated by optical microscope, scanning electron microscope (SEM) with an energy dispersive spectroscope (EDS), and X-ray diffraction (XRD). In as-cast alloys, Al_4RE phase is formed, the content of $Mg_{17}Al_{12}$ phase and the volume fraction of α-Mg phase decrease. In addition, α-Mg phase is refined and the mechanical properties of Mg-9Li-3Al-xRE alloys are improved. However, with increasing mischmetal content, the size of Al_4RE phase increases and the mechanical properties decrease. In extruded alloys, Al_4RE phase is broken into the particles of 1~3 μm in the β-Li matrix phase and α/β interphase. And the best mechanical properties are obtained for Mg-9Li-3Al-1.5RE alloy with a tensile strength of 228.3MPa and elongation of 20.8%, increased by 88.6% and 197.4%, respectively, compared with as-cast Mg-9Li-3Al alloy.

Key words: Mg-Li alloy; mischmetal; extrusion; microstructure; mechanical properties

Mg-Li alloy is one of the lightest metallic structural materials[1-3]. According to the Mg-Li binary phase diagram, Mg-Li alloy possesses α-Mg (hcp) + β-Li (bcc) phase duplex-phase structures at room temperature with Li content between 5.7 wt% to 11.3 wt%[4]. The bcc β-Li matrix phase is soft and ductile, in which the hard α-Mg phase distributed uniformly[5]. Thus the β-Li phase is beneficial to the ductility while α-Mg phase is good for the strength. Hence, the dual-phase Mg-Li alloys usually have better comprehensive mechanical properties than the alloys with single phase (α-Mg or β-Li)[4,5]. However, the mechanical properties of Mg-Li binary alloy is relatively poor which hinder the application in industry[5-10].

Therefore, many methods have been explored for improving the mechanical properties of Mg-Li alloys, such as deformation strengthening, precipitation hardening and alloying strengthening. Strengthening of Mg-Li alloys via the introduction of alloying element represents an effective approach actively being studied and implemented. The frequently used alloying elements include aluminum, zinc, calcium and rare earths[11-13]. As the most common alloying elements, Al and Zn can significantly improve the mechanical properties of Mg-Li alloys due to the solution strengthening and grain refinement[8,14,15].

The mischmetal with lower cost than pure rare earth has been commonly recognized as favorable additives in Mg alloys[16]. The mischmetal have been found in various naturally-occurring proportions, which is also called rare earth mischmetal, Ce mischmetal (rich in Ce), or mischmetal (Mm, rich in La and Ce)[17]. Owing to high thermal stability of mischmetal compound, the addition of La and Ce can increase the hardness, strength and corrosion-resistant of Mg alloys[18-20]. In related studies, Jain and Pettersella[21, 22] revealed that the significant improvement in the high-temperature tensile creep properties of Mg-Al alloys is due to the formation of the fine

rod-like $Al_{11}RE_3$ compound having high thermal stability in the alloys. Moreover, it was reported that the addition of Mm improved slightly the corrosion resistance of AZ91 alloys compared with the addition of Ca[23]. However, the researches about the effects of Mm on the microstructure and mechanical properties of Mg-Li alloys are rarely reported. In this study, the microstructure and mechanical properties of Mg-9Li-3Al-xRE alloys were investigated.

1 Experiment

The alloy ingots with nominal composition of Mg-9Li-3Al-*x*RE (*x*=0, 0.5, 1.0, 1.5, 2.0, wt%) in this study were prepared from commercial pure Mg (99.9%), pure Li (99.9%), pure Al (99.9%) and rare earth elements in a vacuum melting furnace under the protection of argon atmosphere. Mischmetal (Mm) with nominal composition of 45 wt% lanthanum and 55 wt% cerium were added to the melt at 953 K. The melt was maintained at 953 K for 30 min to make sure that the RE could be completely dissolved in the melt. Finally the melt was further homogenized by mechanical stirring and poured into a metal mold with a size of Φ90 mm×100 mm, which was preheated at 523 K. The chemical composition of all as-cast alloys was analyzed by inductively coupled plasma-atomic emission spectroscopy (ICP-AES), and the results are shown in Table 1. The as-cast specimens were machined from Φ90 to Φ80 mm. A homogenizing treatment was carried out at 523 K for 12 h and then the specimens were extruded at 523 K with extrusion ratio of 32.

The specimens for microstructure observation, which were cut from the same positions of both the initial ingots and extruded samples, were polished and etched in a solution of 4 vol% nital. Microstructure observations were performed on the optical microscope (Olympus), scanning electron microscope (SEM, JOEL/JSM-6460LV) with an energy dispersive spectroscope (EDS, Oxford). Moreover, the constituent phase of the specimens was identified by X-ray diffraction (XRD, D/MAX-A). Tensile tests of all specimens were conducted at room temperature on a CMT-5105 (SANS Materials Analysis Inc., Shenzhen, China) tensile tester with a crosshead speed of 0.5 mm/min.

2 Results and Discussion

2.1 Microstructure of Mg-9Li-3Al-*x*RE alloys

Fig.1 shows XRD patterns of as-cast alloys. Mg-9Li-3Al alloy consists of α-Mg, β-Li and $Mg_{17}Al_{12}$ phases. After adding RE, the Al_4RE intermetallic phase is formed in Mg-9Li-3Al-*x*Re alloys. With the increase of RE content, the diffraction peaks of Al_4RE phase increase gradually, whereas the diffraction peaks of $Mg_{17}Al_{12}$ phase decrease. The formation energy of intermetallic compound depends on the difference in electronegativity of the two elements[24]. Since the difference in electronegativity between Al and RE (EN=0.5) is bigger than that between Al and Mg (EN=0.2), thus rare earths are prone to

Table 1   Chemical compositions of the as-cast alloys (wt%)

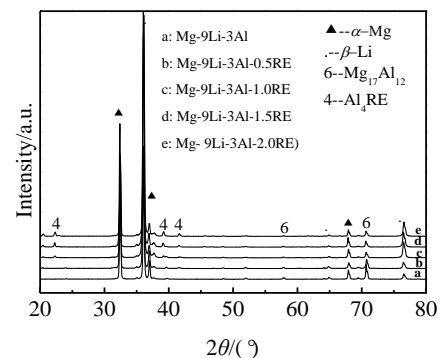| As-cast alloys	Li	Al	La	Ce	Mg
Mg-9Li	8.96	-	-	-	Bal.
Mg-9Li-3Al	8.83	3.03	-	-	Bal.
Mg-9Li-3Al-0.5RE	8.92	3.04	0.23	0.24	Bal.
Mg-9Li-3Al-1.0RE	8.76	2.93	0.47	0.44	Bal.
Mg-9Li-3Al-1.5RE	9.15	3.06	0.75	0.74	Bal.
Mg-9Li-3Al-2.0RE	9.12	2.98	0.99	0.98	Bal.

Fig.1   XRD patterns of Mg-9Li-3Al-*x*RE alloys

react with Al. As a result, the Al_4RE phase with high chemical stability is more likely to be formed instead of pseudobinary Mg-RE phase or pseudoternary Mg-Al-RE phase[23]. With increasing RE addition, the more Al_4RE phases are formed, which further suppress the formation of $Mg_{17}Al_{12}$ phase[17,25,26].

The optical micrographs of the as-cast Mg-9Li-3Al-*x*RE alloys are shown in Fig.2. It can be seen from Fig.2a that the as-cast Mg-9Li alloy possesses a dual-phase microstructure, consisting of α-Mg phase with petal-like shape distributed in the β-Li matrix. After adding Al, some black particles are found along the interfaces of α-Mg phase and β-Li matrix in Fig.2b. A previous study indicated that the particles should be $Mg_{17}Al_{12}$ phases[8]. Moreover, this conclusion can be confirmed by Fig.1. With the addition of RE into Mg-9Li-3Al, some rod-like and point-like intermetallic Al_4RE can be observed along the α/β interface and within β-Li matrix as shown in Fig.2c~2f. Moreover, the number of rod-like phase increases significantly and the morphology becomes more continuous with increasing RE addition. Furthermore, when the content of RE is excessive, the amount and the size of α-Mg phase also can decrease, as shown in Fig.2. As the RE content increases to 2.0 wt%, it can be seen that the volume fraction of β-Li phase increases from 50.8 vol% to 64.7 vol% according to Fig.3. The area percent (S_β) of β-Li phase was calculated by Image-Pro Plus™ for three times and the mean values were calculated for different alloys. According to the method of weighted mean, the volume fraction (V_β) of α-Mg is
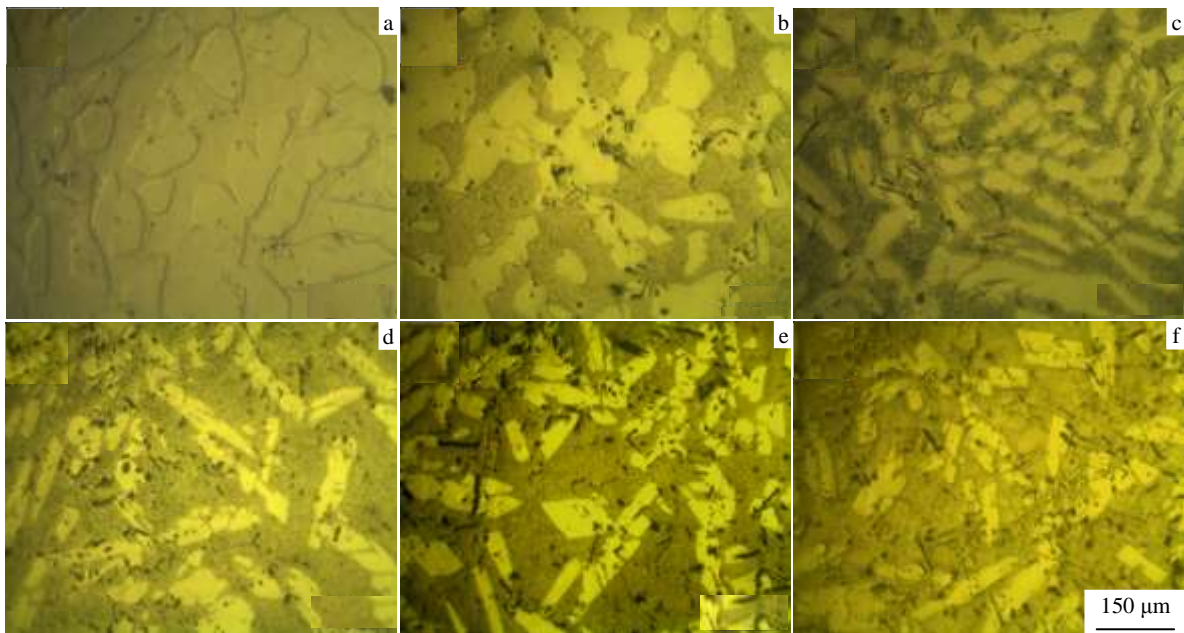
Fig.2   Optical micrographs of the as-cast Mg-Li alloys: (a) Mg-9Li, (b) Mg-9Li-3Al, (c) Mg-9Li-3Al-0.5RE, (d) Mg-9Li-3Al- 1.0RE, (e) Mg-9Li-3Al-1.5RE, and (f) Mg-9Li-3Al-2.0RE

evaluated using Eq.(1):

$$V_\beta = \frac{(\sqrt{s_\beta})^3}{(\sqrt{s_\alpha})^3 + (\sqrt{s_\beta})^3 + (\sqrt{s_{Al_4RE}})^3} \quad (1)$$

where S_α is the area percent of α-Mg phase, and S_{Al_4RE} is the area percent of Al_4RE compounds.

Wu et al [10] discovered that the additions of Al and Y restrained the α-Mg phase in the dual-phase Mg-8Li-(1,3)Al alloy. The similar phenomenon that the eutectic pockets (Mg_3Zn_6Y) prevented the homogenous diffusion of Li atom during the solidification can be observed in Mg-6Li-6Zn-1.2Y alloy[27]. It can be seen from Fig.3 that the volume fraction of β-Li phase in Mg-9Li and Mg-9Li-3Al has no obvious change. When the content of RE is 0.5 wt%, the volume fraction of

Fig.4   SEM image (a) and EDS spectrum (b) of Al_4RE phase in Mg-9Li-3Al-1.5RE alloy

β-Li phase begins to increase significantly. It suggests that the $Mg_{17}Al_{12}$ phase has little effect on the volume fraction of β-Li phase, but the new rare earth compounds Al_4RE, as well as Al_2Y and Mg_3Zn_6Y, have the same refineing effect that can restrain the homogenous diffusion of Li and the growth of
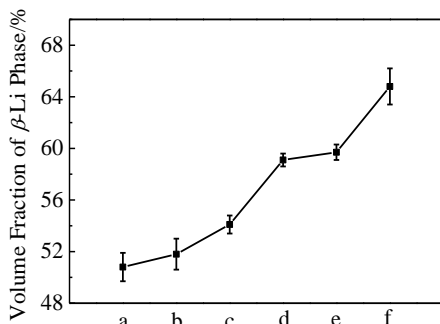

Fig.3   Volume fraction of β-Li in as-cast Mg-Li alloys (a: Mg-9Li, b: Mg-9Li-3Al, c: Mg-9Li-3Al-0.5RE, d: Mg-9Li-3Al-1.0RE, e: Mg-9Li-3Al-1.5RE, f: Mg-9Li-3Al-2.0RE)
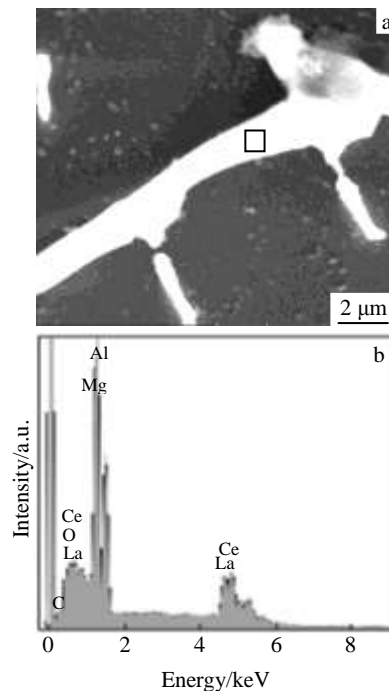
α-Mg phase. Fig. 4 shows that the SEM and EDS result of Al₄RE phase in Mg-9Li-3Al-1.5RE alloy. The EDS results combined with XRD analysis, confirm that the composition of white blocky compounds is mainly Mg, Al, La and Ce. The main reason for the presence of O is the oxidization of Mg-Li alloy. The impurity element C was introduced by graphite crucible. Since the solid solubility of La and Ce in Mg matrix is only 0.14% and 0.09%, respectively, it is possible that Mm can be as the heterogeneous nucleation for phase refinement in Mg-Li alloy[28]. During the solidification process, the solute atoms Mm are enriched in the front of the S/L interface, and this could result in constitutional supercooling and promotion of heterogeneous nucleation[29]. Otherwise, Based on Jiang's[25] research of edge-to-edge matching model, the low misfit and mismatch values between Al₄Ce and Mg suggest that Al₄Ce is an effective grain refiner for Mg alloys. And according to the XRD PDF (#65-2678-Al₄Ce, #65-2679-Al₄La), Al₄La and Al₄Ce have the same crystal structure as tetragonal with space group I4/mmm. It can be known that the main reason that the size of α-Mg phase decreased is the refinement of Al₄RE.

In the present work, it indicates that mischmetal La/Ce has bigger effect than Ce or La on the grain refinement of Mg-Li-based alloy[30]. The addition of mischmetal La/Ce can interact and reduce the solid solubility in α-Mg phase, which result in the enrichment of La and Ce in the solid-liquid interface. The enrichment of La and Ce would lead to more effective undercooling refining effect[31]. Moreover, the size, shape, quantity and distribution of secondary phases in the alloy with added mischmetal La/Ce is different from that of

the alloy added La or Ce only. It can be seen that the morphology of Al₄RE particles is short rod-like and point-like from Fig.2. However, the microstructure of as-cast Mg-8Li-1Al-1Ce alloy is composed of α-Mg phase, β-Li phase and long rod-like precipitated compound[32]. It indicates that the secondary phases of the alloy with added mischmetal La/Ce are finer and more uniform than those of the alloy with added La or Ce separately. It can be more effective on the grain- boundary strengthening. The same phenomenon happened in Mg-5Al-Sr alloy. In as-cast Mg-5Al-1Sr alloy, Al₄Sr particles changed from coarse plate at grain boundaries into fine polygonal or short rod with the additions of titanium. Furthermore, the Al₄Sr particles distributed more uniformly and the amount of lamellar Al₄Sr phase was greatly decreased[33]. Thus, the refinement effect of mischmetal La/Ce is more obvious than that of single La or Ce.

Fig.5c shows the optical micrographs of extruded Mg-9Li-3Al-1.5RE alloy along the extrusion direction. It can be seen that the phases and intermetallic compounds in the extruded alloys are much finer than that in as-cast alloys. After extrusion, the size of α-Mg phases are refined from 150~200 μm to 10~20 μm. Moreover, the rod-like Al₄RE phase is broken into particles of 1~3 μm and homogeneously distributed in β-Li matrix and α/β interphase. It is conducive to strength of β-Li matrix and further improves the mechanical properties of the extruded alloys.

2.2 Mechanical properties of Mg-9Li-3Al-xRE alloys

Fig.6 shows the mechanical properties of as-cast and extruded alloys at room temperature. The results show that the
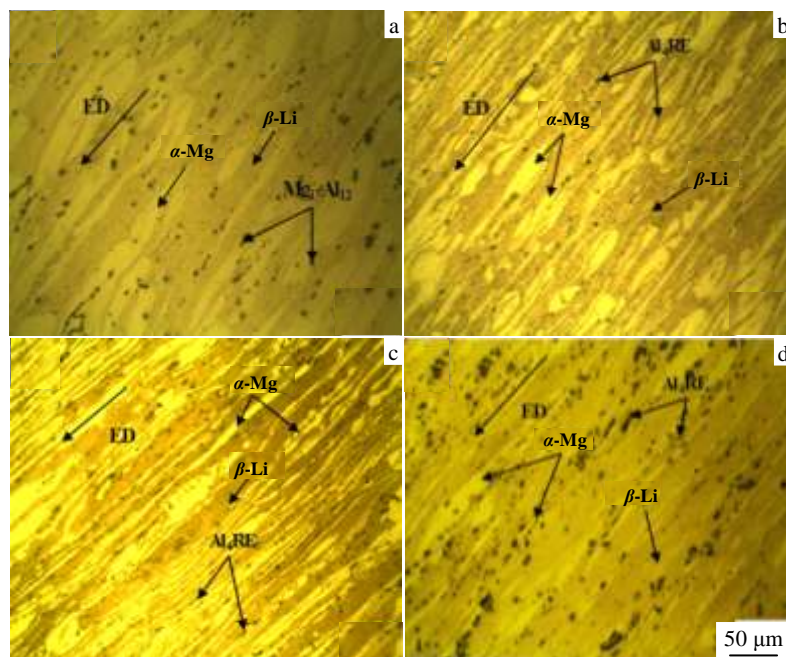

Fig.5   Optical micrograph of as-extruded Mg-9Li-3Al-*x*RE alloys: (a) *x*=0, (b) *x*=0.5, (c) *x*=1.5, and (d) *x*=2.0
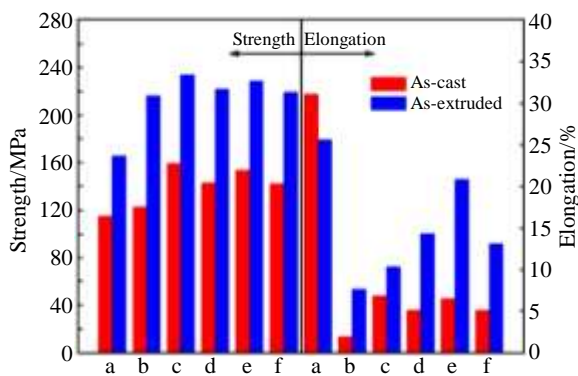
Fig.6 Mechanical properties of Mg-Li alloys (a: Mg-9Li, b: Mg-9Li-3Al, c: Mg-9Li-3Al-0.5RE, d: Mg-9Li-3Al-1.0RE, e: Mg-9Li-3Al-1.5RE, f: Mg-9Li-3Al-2.0RE)

as-cast and extruded Mg-9Li alloys possess better ductility than other Mg-Li alloys. The principal reasons are as follows: Firstly, only the basal slip (0001) $<11\bar{2}0>$ plays the dominant role during the deformation in α-Mg phase with hcp structure at room temperature. However, the β-Li phase with bcc structure has more active slip systems than α-Mg phase with hcp structure[4, 34]. The addition of Li leads to the reduction of c/a axial ratio of the hcp lattice so that the sliding systems are easy to activate [4], such improving the deformability of dual-phase Mg-Li alloy.

As shown in Fig.6, the extruded Mg-Li alloys have a favorable combination of tensile strength and ductility. These favorable properties are definitely related to special microstructure of dual phase in Mg-Li alloy, in which the soft β-Li matrix provides good ductility; meanwhile the hard α-Mg phase plays the load-bearing role. In fact, this microstructure is similar to that of some kind of metallic composite. After extrusion, the shape of α-Mg phase becomes long strip under the compression stress along the extruding direction. It can be seen that the extruded structures of all alloys exhibit fibrous extruding texture, which are typical plastically deformed structures, just like "fiber-reinforced composite", as shown in Fig.5.

According to Fig.6, the tensile strength of the Mg-9Li alloy increases from 115.2 MPa to 167.6 MPa, but the elongation decreases from 32.2% to 26.3% after extrusion. The main reason for the increment of the tensile strength of extruded Mg-9Li alloy might be the uniform distribution of the fiber of α-Mg phases in the β-Li matrix. Moreover, it can be seen that the tensile strength of Mg-9Li-3Al-xRE alloy is improved significantly compared with Mg-9Li alloy. The improvement of tensile strength is mainly attributed to grain refinement strengthening and second phase strengthening. First, the grain size of Mg-9Li-3Al-xRE alloy is finer than that of Mg-9Li alloy, so the tensile strength and elongation of Mg-9Li-3Al-xRE alloy are enhanced by grain refinement

strengthening effect. On the other hand, as the second phase particles, the Al_4RE compounds are located at the α/β interphase and in the β-Li matrix. It is considered to be an effective obstacle to grain boundary sliding and dislocation motion in the vicinity of the grain boundaries during the deformation. Compared with the as-cast alloys, the extruded alloys have better comprehensive mechanical properties. It indicates that extrusion plays an important role in the improvement of mechanical properties.

The ultimate tensile strength of as-cast and extruded Mg-9Li-3Al alloy is 119.6 MPa and 218.3 MPa, respectively. Compared with Mg-9Li-3Al alloy, the ultimate tensile strength of as-cast and extruded Mg-9Li-3Al-0.5RE alloy reaches 159.7 MPa and 234.7 MPa, increased by 33.5% and 27.7%, respectively. When the content of RE is 1.5 wt%, the Mg-9Li-3Al-1.5RE alloy represents the best comprehensive mechanical properties. Compared with as-cast Mg-9Li-3Al alloy, the ultimate tensile strength and elongation of extruded Mg-9Li-3Al-1.5RE alloy are 228.3MPa and 20.8% at room temperature, increased by 88.6% and 197.4%, respectively. The extrusion can result in grain refinement and the formation of more grain boundaries. The former can make deformation more uniform because the stress can be dispersed to the more grains. And the latter can effectively hinder dislocation sliding since it is difficult to go through grain boundaries for dislocation. Thus extrusion can improve the plasticity and strength. Moreover, the strain hardening in the process of extrusion also can enhance the strength. When RE content reaches to 2 wt%, the coarse Al_4RE phase is formed, which is a disadvantage for the mechanical properties, especially the elongation.

As mentioned before, with the addition of Mm, the volume fraction of β-Li phase increases and the strengthening effect of α-Mg weaken. But the strength of Mg-9Li-3Al-xRE increases since the Al_4RE compounds are dispersed in β-Li matrix. It indicates that the strengthening effect of the Mm can offset the negative effect of the volume fraction reduction of α-Mg phase. It is worth noting that the Mm is a favorable factor for improving the strengthening and elongation.

2.3 Failure analysis and fractography

SEM images of tensile fracture surface of the extruded Mg-9Li and Mg-9Li-3Al-xRE alloys are shown in Fig.7, which exhibit mixed characteristics of cleavage and ductile fractures that belong to quasi-cleavage fracture. A large number of plastic dimples and some cleavage steps can be found on the fracture surface. With increasing the Mm content, the size of dimples decreases sharply. Generally, smaller and deeper plastic dimples can prove that as-extruded Mg-9Li-3Al-1.5RE alloy possesses good ductility during the tensile testing. When the content of Mm is 2 wt%, some coarse Al_4RE particles are observed at the bottom of the dimples which maybe become the origin of cracks between the second-phase and the matrix.
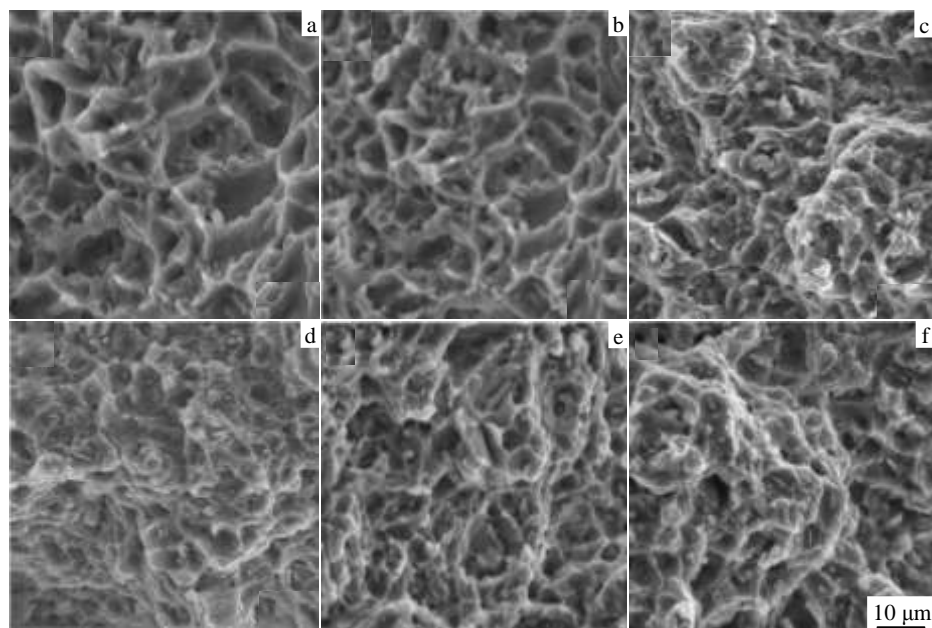
Fig.7   Typical tensile fracture morphologies of as-extruded Mg-9Li alloy (a) and Mg-9Li-3Al-*x*RE alloys: (b) *x*=0, (c) *x*=0.5, (d) *x*=1.0, (e) *x*=1.5, and (f) *x*=2.0

3   Conclusions

1) Mg-9Li-3Al-*x*RE alloy consists of *α*-Mg, *β*-Li, Al$_4$RE and Mg$_{17}$Al$_{12}$ phases. The Al$_4$RE phase is mainly distributed at the *α/β* interface and in *β*-Li matrix in as-cast alloys.

2) With increasing of the RE content, the *α*-Mg phase is refined due to lower misfit and mismatch values between Al$_4$RE and Mg. After extrusion, the rod-like Al$_4$RE phase is broken into fine particles with approximately 1~3 μm.

3) The refinement effect of mischmetal La/Ce is more obvious than single La or Ce.

4) When addition of RE reaches 2 wt%, the optimal tensile strength and ductility are obtained simultaneously. Compared with as-cast Mg-9Li-3Al alloy, the strength and elongation reach 228.3 MPa and 20.8% at room temperature, increased by 88.6% and 197.4%, respectively.

References

1   Zheng X F, Peng X D, Li J C *et al. Rare Metal Materials and Engineering*[J], 2014, 43(9): 2079

2   Xu T C, Peng X D, Jiang J W *et al. Rare Metal Materials and Engineering*[J], 2014, 43(8): 1815

3   Zeng Ying, Jiang Ying, Huang Dehui *et al. Journal of Magnesium and Alloys*[J], 2013(1): 297

4   Yang Yan, Peng Xiaodong, Wen Haiming *et al. Metallurgical and Materials Transactions A*[J], 2013, 44: 1101

5   Cheng Liren, Cao Zhanyi, Wu Ruizhi *et al. Materials Transactions*[J], 2010, 51: 1526

6   Takuda H, Matsusaka H, Kikuchi S *et al. Journal of Materials Science*[J], 2002, 37: 51

7   Liu T, Zhang W, Wu S D *et al. Materials Science and Engineering A*[J], 2003, 360: 345

8   Drozd Z, Trojanová Z, Kúdela Z *et al. Journal of Alloys and Compounds*[J], 2004, 378: 19

9   Song G S, Staiger M, Kral M. *Materials Science and Engineering A*[J], 2004, 371: 371

10   Wu Ruizhi, Qu Zhikun, Zhang Milin. *Materials Science and Engineering A*[J], 2009, 516: 96

11   Huang Y, Gan W, Kainer K U *et al. Journal of Magnesium and Alloys*[J], 2014(2): 1

12   Gao Lei, Yan Hong, Luo Jun *et al. Journal of Magnesium and Alloys*[J], 2013, 1: 283

13   Chang H W, Qiu D, Taylor J A *et al. Journal of Magnesium and Alloys*[J], 2013, 1: 115

14   Chang Tienchan, Wang Jianyih, Chu Chunlen *et al. Materials Letters*[J], 2006, 60: 3272

15   Yan Hong, Chen Rongshi, Han Enhou. *Transactions of Nonferrous Metals Society of China*[J], 2010, 20: 550

16   Wu R Z, Qu Z K, Zhang M L. *Reviews on Advanced Materials Science*[J], 2010, 24: 35

17   Nam N D, Kim W C, Kim J G *et al. Corrosion Science*[J], 2009, 51: 2942

18   Moosa A A. *Al-Khwarizmi Engineering Journal*[J], 2011(7): 75

19   Xiao Wenlong, Jia Shusheng, Wang Jianli *et al. Acta Materialia*[J], 2008, 56: 934

20   Wang Jianli, Peng Qiuming, Wu Yaoming *et al. Transactions of Nonferrous Metals Society of China*[J], 2006, 16: 1703

21   Jain C C, Koo C H. *Materials Transactions*[J], 2006, 47: 433

22   Pettersell G, Westengen H, Hoier R *et al. Materials Science and Engineering A*[J], 1996, 207: 115

23 Wu Guohua, Fan Yu, Gao Hongtao *et al. Materials Science and Engineering A*[J], 2005, 408: 255

24 Miedema A R, Boer F R, Chatel P F. *Journal of Physics F: Metal Physics*[J], 1973, 3: 1558

25 Jiang Bin, Zeng Ying, Zhang Mingxing *et al. Journal of Materials Research*[J], 2013, 28: 2694

26 Zhang S, Wei B, Lin H *et al. The Chinese Journal of Nonferrous Metals*[J], 2001, 11: 99 (in Chinese)

27 Xu D K, Zu T T, Yin M *et al. Journal of Alloys and Compounds*[J], 2014, 582: 161

28 Rokhlin L L. *Journal of Phase Equilibria*[J], 1995, 16: 504

29 Li Shuangshou, Zheng Weichao, Tang Bin *et al. Journal of Rare Earths*[J], 2007, 25: 227

30 Wu R Z, Deng Y S, Zhang M L. *Journal of Materials Science*[J], 2009, 44: 4132

31 Zhang Jinghuai, Zhang Deping, Tian Zheng *et al. Materials Science and Engineering A*[J], 2008, 489: 113

32 Wang Tao, Zhang Milin, Wu Ruizhi. *Materials Letters*[J], 2008, 62: 1846

33 Zhao Peng, Wang Qudong, Zhai Chunquan *et al. Materials Science and Engineering A*[J], 2007, 444: 318

34 Suresh K, Rao K P, Prasad Y V, Hort N *et al. JOM*[J], 2013, 66: 322

混合稀土对超轻 Mg-Li 合金微观组织和力学性能的影响

李杨敏 [1]，彭晓东 [1,2]，胡发平 [1]，魏国兵 [1]，谢卫东 [1,2]，刘军威 [1]，杨　艳 [1]，李孟孪 [1]，王雪梅 [3]

(1. 重庆大学材料科学与工程学院，重庆 400044)

(2. 国家镁合金材料工程技术研究中心，重庆 400044)

(3. 上汽依维柯红岩商用车有限公司，重庆 401122)

摘　要：对 La/Ce 混合稀土的 Mg-9Li-3Al-xRE (x=0, 0.5, 1, 1.5, 2, 质量分数，%) 合金，利用光学显微镜，带能谱（EDS）的扫描电子显微镜（SEM）和 X 射线衍射（XRD）研究了微观组织对其力学性能的影响。结果表明，在加入混合稀土的铸态合金中，形成了 Al_4RE 相，并且 $Mg_{17}Al_{12}$ 相的含量和 α-Mg 相的体积分数均被减少。此外，细化了 α-Mg 相并提高了合金的力学性能。但是，随着 La/Ce 混合稀土含量的增加，Al_4RE 相的尺寸增大，降低了合金的力学性能。在加入混合稀土的挤压态合金中，合金中 Al_4RE 相挤压破碎至 1~3 μm，分布于 β-Li 基体中和 α/β 相之间。Mg-9Li-3Al-1.5RE 合金获得最好的力学性能，最大抗拉强度和延伸率分别为 228.3 MPa 和 20.8%，同铸态 Mg-9Li-3Al 相比分别提高了 88.6% 和 197.4%。

关键词：Mg-Li 合金；混合稀土；挤压；微观组织；力学性能

作者简介：李杨敏，男，1988 年生，硕士，重庆大学材料科学与工程学院，重庆 400044，电话：023-65106774，E-mail: 20093960@cqu.edu.cn